CISPR/A/WG1 LLAS tables (Beeckman)16-01

For IEC use only

2016-07-21

INTERNATIONAL ELECTROTECHNICAL COMMISSION

INTERNATIONAL SPECIAL COMMITTEE ON RADIO INTERFERENCE (CISPR)

CISPR A WG 1: EMC instrumentation specifications

Subject:

Updated LLAS model and amended figures and tabular values of LLAS figures in Annex C of CISPR 16-1-4

Foreword:

During the CISPR A WG1 of 2015 meeting in Stresa [f1] a number of papers were presented and discussed on the model and validation factor of the large loop antenna system (LLAS)[f1][f3][f4][f5].

The paper by Mr. Beeckman [f1] introduced the LLAS-model and existing tabular values for conversion and validation factors based on the original work by Van Veen and Bergervoet. In addition, the proposed changes to Annex C of CISPR 16-1-4 and relevant background information for inclusion in CISPR TR 16-3 was proposed. Also two papers by Mr. Midori et al were presented [f3][f4]. Both papers by Midori [f3][f4] introduced an alternative LAS model based on the application of a Neumann integral for calculation of the mutual inductance between the loops of the LLAS and the calibration dipole and NEC2 calculation for calculating the validation factor. Also the changes required in CISPR 16-1-4 were identified. The application of the more accurate value of the mutual inductance results in a reduction of the validation factor of approximately 1,6 dB, which is quite significant. However, verification measurements shown by Mr. Schwarzbeck using results of measured data of 24 LLAS units [f5], and verification results reported by Mr. Midori in a later paper [f6] show that the validation curve with the 1,6 dB shift provides a better match with actual LLAS units in the field. From these verification tests it was also concluded that the current acceptance criterion of ±2 dB is hardly to meet now in practice. As a consequence, it was proposed to increase the tolerance for the validation factor from ±2 dB to ±3 dB.

After the discussion at the CISPR A WG1 meeting in Stresa [f1] the following was decided:

1) To upgrade the model of the LLAS based by applying the more accurate value of the mutual inductance and to achieve a better match of the validation factor in practice
2) To recalculate the curves and tabular values of the validation factor
3) To change the tolerance of the validation factor from ±2 dB to ± 3 dB

It was agreed (action Item 15-04 of the WG1-Stresa meeting minutes) to revise the proposal on conversion and validation factors for large loop antenna and to circulate it to the WG1.

The attached paper is an updated version of [f2]. It describes the modified model of the LLAS that includes the abovementioned modifications agreed at the WG1 meeting in Stresa [f1]. Also the modified tabular values for the validation factor have been calculated as a function of frequency.

Annex A gives the proposed changes in Annex C of CISPR 16-1-4 that are needed to incorporate the new curves for the validation factor and the conversion factors and the tabular values of the curves in question. Also the new acceptance criterion is introduced. It is proposed to submit this Annex A as a DC to the National Committees.

In view of the increased relevance of magnetic field measurement methods below 30 MHz, it is proposed to add the results of this work also as background material in CISPR TR 16-3.

WG1 Papers referenced:

[f1] CISPR/A/WG1(Secretary)15-03, *Unconfirmed minutes of the meeting of Working Group 1 of CISPR/A, held in Stresa, Italy on September 24*, November 20, 2015.
[f2] CISPR/A/WG1 LAS tables (Beeckman)15-01, *LAS model and tabular values of LLA figures in Annex C of CISPR 16-1-4*, 2015-01-21.
[f3] CISPR/A/WG1 LAS Tables (Midori-Kurihara-Fujii-Shinozuka)15-01, *Proposal of tabular values of validation factor for LAS*, February 2015.
[f4] CISPR/A/WG1 LAS Tables (Midori-McLean-Kurihara-Fujii-Shinozuka)15-02, *Proposal of tabular values of validation factor and conversion factor for LAS*, August 2015.
[f5] Paper Schwarzbeck, Loop Antenna System CISPR 16-1-4 Ed. 3.
[f6] CISPR/A/WG1 LAS Tables (Midori-Kurihara-Fujii-Shinozuka)15-04, *Verification of the calculation model of validation factor and the tolerance of validation factor for LAS*, January 2016.

1 Introduction

The attached paper is an updated version of [1]. It describes the modified model of the LLAS that includes the modifications agreed at the WG1 meeting in Stresa. Also the modified tabular values have been calculated as a function of frequency.

The various curves presented by Figure C.8, Figure C.10 and Figure C.11 of CISPR 16-1-4 [2] are to be replicated and are to be presented in tabular form.

The curves in question have been derived from the EMC Zurich conference paper by Bergervoet and Van Veen [3], the inventors of the LLAS. The latter paper has also been referenced in the bibliography of CISPR 16-1-4 i.e. bibliographic reference [11].

This paper contains all the necessary equations for calculating the curves of the before mentioned figures.

In this paper the models and equations are given to replicate the following figures:

– Figure C.11: Sensitivity SD of a large-loop antenna with diameter D relative to a large-loop antenna having a diameter of 2 m;

– Figure C.8: Validation factor for a large loop-antenna of 2 m diameter;

– Figure C.10: Conversion factors C_{dA} [for conversion into dB(µA/m)] and C_{dV} (for conversion into dB(µV/m)) for two standardized measuring distances d .

Subsequently for each curve also tabular values are given.

2 Response of a LAS to a magnetic field dipole

2.1 Magnetic field model of a disturbance source

Equipment under test (EUT) that contains a magnetic field disturbance source is represented by a circular loop with radius R (diameter D) that carries a sinusoidal varying current I (frequency f). See Figure 1.

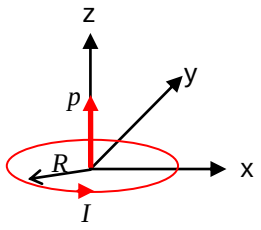

Figure 1 – Geometry and coordination system for a single magnetic dipole

The magnetic field disturbance source can be represented by its magnetic field dipole moment p as follows:

$$p = S \cdot I = \pi R^2 \cdot I \quad \text{in Am}^2 \tag{1}$$

where

S is the surface of the disturbance loop of the EUT in m^2,

I is the disturbance current through loop of the EUT (in A).

2.2 Response of a LAS to a magnetic dipole

2.2.1 Relation LLAS-current and EUT-current using the transformer model

The configuration of an EUT in the centre of a LLAS is depicted in Figure 2. In the remainder of this paper it is assumed that the loops of the disturbance source of the EUT and the LLAS loop are coaxially positioned in the same plane. The current measured in the LLAS is proportional with the magnetic dipole moment of the EUT. Theoretical details are given in the paper of Bergervoet and Van Veen [3]. Also more recent papers of McLean et al [4][5], give the model and equations of the LLAS.

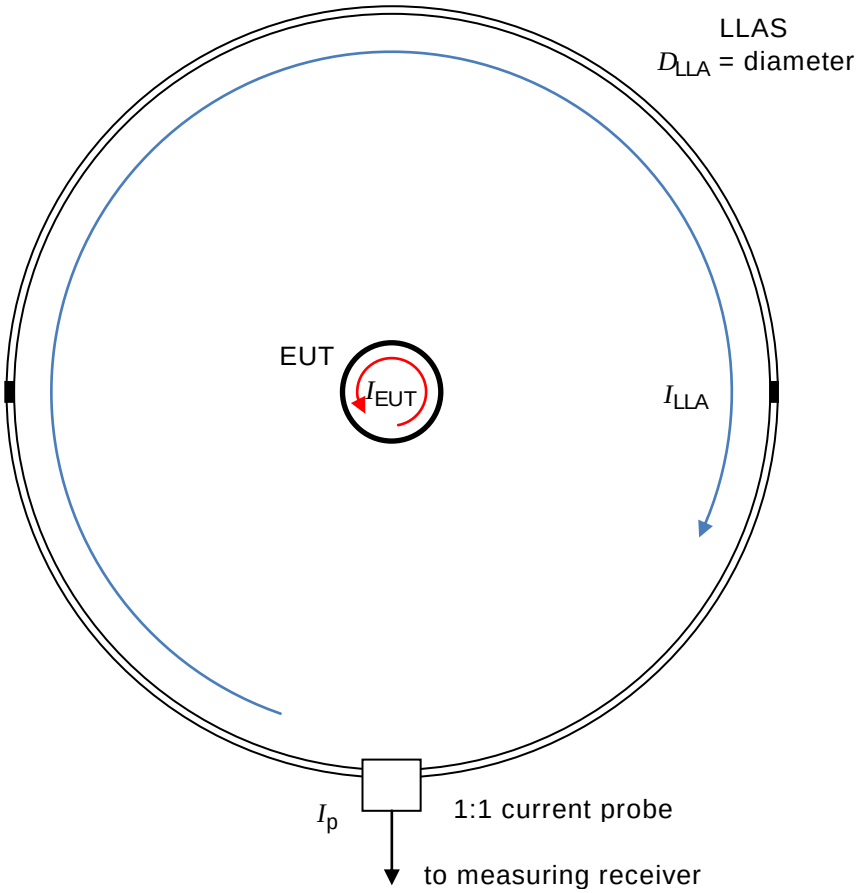

Figure 2 – Configuration measurement an EUT in an LLAS with two gaps

This configuration can be considered as a loosely coupled loop transformer. Then the current I_{LLA} in a short-circuited LLAS corresponds with the magnetic dipole moment p_{EUT} of the EUT as follows (equation (2) of [3]):

$$I_{LLA} = \frac{\mu_0}{D_{LLA} L_{LLA}} \cdot p_{EUT} \tag{2}$$

where,

D_{LLA} the diameter of the LLAS in meters,

L_{LLA} is the inductance of the LLAS in Henry.

The inductance of the LLAS-loop is accurately given by the following equation:

$$L_{\mathrm{LLA}} = \frac{\mu_0}{2} \cdot D_{\mathrm{LLA}} \left\{ \ln\left(\frac{8D_{\mathrm{LLA}}}{d_{\mathrm{LLA}}} \right) - 2 \right\} \tag{3}$$

where d_{LLA} is the diameter of the LLAS-loop wire in meters (see equation (3) of [3]).

For the LLAS, this concerns the outer diameter of the shield of the coaxial cable. In case of RG-223/U, d_{LLA} = 3,96 mm.

For a 2m LLAS, the inductance L_{LLA} is:

$$L_{\mathrm{LLA}} \text{ (2m LLAS)} = 7{,}92\ \mu\mathrm{H} \tag{4}$$

As mentioned before, the two coupled loops can be represented by a loosely coupled loop transformer. The network then can be represented as shown in Figure 3. This gives the following ratio (absolute value) of the LLAS current and the disturbance current:

$$\frac{I_{\mathrm{LLA}}}{I_{\mathrm{EUT}}} = \frac{M}{L_{\mathrm{LLA}}} \tag{5}$$

where M is the mutual inductance between the two circular co-axial loops given by:

$$M = \frac{\mu_0 S}{D_{\mathrm{LLA}}} = \frac{\mu_0 \pi R^2}{D_{\mathrm{LLA}}} \tag{6}$$

The mutual inductance M is simply determined by the sizes of the two coaxial loops.

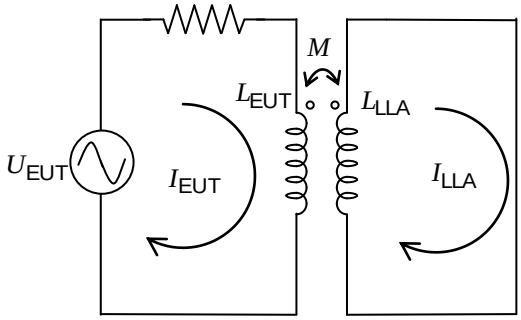

Figure 3 – Transformer model representation of a disturbance source inside a LLAS antenna

2.2.2 Relation LLAS-current and measured signal by the 1 V/A current probe

The current in the loop antenna is measured using a 1 V/A current probe as specified in CISPR 16-1-4. The LLAS specified in CISPR 16-1-4, is not a single short-circuited loop. The LLAS consists of two semi-circles of coaxial cables which are interconnected and terminated in a specific way. In this way the LLAS can be modelled as two parallel coaxial cables terminated with 50 Ω resistors (two 100 Ω resistors in parallel). This two slit configuration gives a flat frequency response over the frequency range of interest (9 kHz – 30 MHz) and provides shielding against electric field. The transfer function giving the current I_{p} measured by the 1 V/A current probe in terms of the loop current is given by equation (11) of [3]. The equation, also given in [4], is used:

$$f_c(\omega) = \frac{I_p}{I_{LLA}} = j\left[\frac{R_C}{R_T}\sin\left(\frac{k_C \pi R_{LLA}}{2}\right) - j\cos\left(\frac{k_C \pi R_{LLA}}{2}\right) - j\frac{R_C}{R_A}\frac{\sin\left(\frac{k_C \pi R_{LLA}}{2}\right)}{\tan\left(\frac{k \pi R_{LLA}}{2}\right)}\right]^{-1} \quad (7)$$

where

j is the complex number (time dependence $e^{j\omega t}$ is used here, instead of $e^{-j\omega t}$ in [3]),

k is the free-space wave impedance = $\frac{2\pi}{\lambda}$,

k_C is the wave number inside the dielectric of the coaxial cable = $\frac{2\pi}{\lambda_c} = \frac{k}{v_c}$, where

v_c is the signal speed relative to the speed of light inside the coaxial cable = $1/\sqrt{\varepsilon_r}$ = 0,67 for PTFE dielectric of an RG-223/U cable,

λ_c is the wavelength inside the dielectric of the coaxial cable,

R_C is the characteristic impedance of the LLAS-coaxial cable = 50 Ω (RG-223/U),

R_T is the termination impedance of the LLAS-coaxial cable = 50 Ω (two 100 Ω in parallel),

R_A is the per-unit length inductance of LLAS-coaxial cable times speed of light:

$$R_A = L_{LLA}\frac{c}{2\pi R_{LLA}} = \frac{\mu_0 c}{2\pi}\cdot D_{LLA}\left\{\ln\left(\frac{8D_{LLA}}{d_{LLA}}\right) - 2\right\} \quad (8)$$

Hence, combining the equations (2) and (7) gives the measured current:

$$I_p = \frac{\mu_0}{D_{LLA} L_{LLA}}\cdot f_c(\omega)\cdot p_{EUT} \quad (9)$$

In Figure 4 the transfer function $f_c(\omega)$ is given as a function of frequency for a 2 m LLAS.

The transfer function is constant for a large part of the frequency range of interest. For low frequencies the transfer function becomes:

$$\lim_{\omega\to 0} f_c(\omega) = \frac{R_A}{R_A + R_C / v_c} = 0{,}835 \quad (10)$$

Expressed in dB the mismatch factor is -1,57 dB.

2.2.3 Near-field effect

The influence of the near-field of the disturbance source requires an additional correction factor to equation (9). In the original paper of Bergervoet [3] the influence of the near field of the disturbance source is taken into account by an additional correction factor $g_c(\omega)$ which applies for an LLAS and EUT in free-space:

$$I_p = \frac{\mu_0}{D_{LLA} L_{LLA}}\cdot f_c(\omega)\cdot g_c(\omega)\cdot p_{EUT} \quad (11)$$

where

$$g_c(\omega) = 1 - jkD_{LLA}/2 \tag{12}$$

NOTE In the original paper of Bergervoet [3] an error is present in equation (16) of the paper, i.e. the radius of the LLAS is missing in the second term of the equation.

Equation (11) can be simplified by using equations (1) and (6):

$$\frac{I_p}{I_{EUT}} = \frac{M}{L_{LLA}} \cdot f_c(\omega) \cdot g_c(\omega) \tag{13}$$

In Figure 4 the transfer function $g_c(\omega)$ is given as a function of frequency for a 2 m LLAS. Also the overall transfer function $f_c(\omega) \cdot g_c(\omega)$ is given in this Figure 4.

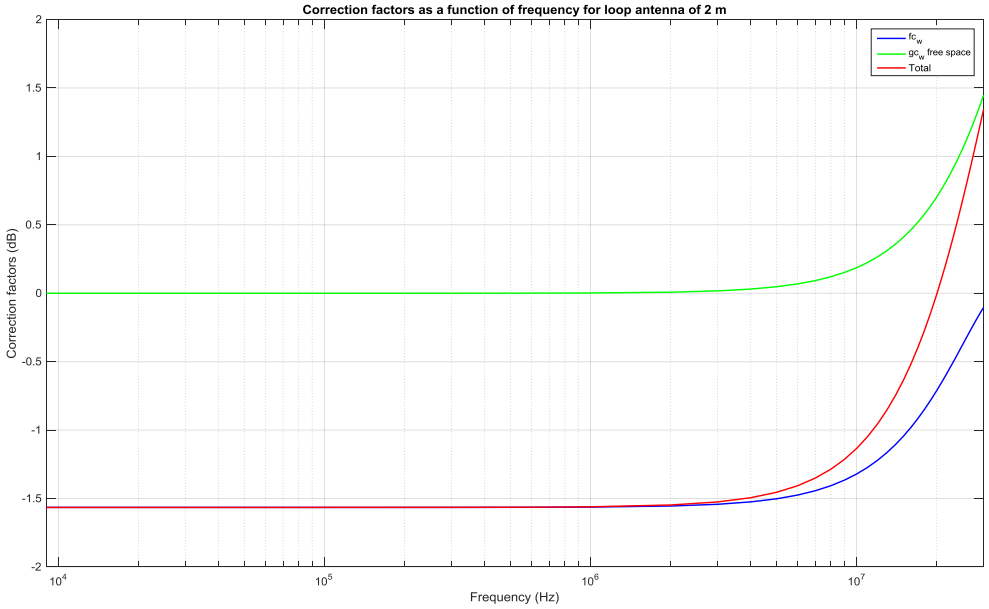

Figure 4 – Transfer functions $f_c(\omega)$ and $g_c(\omega)$ as a function of frequency for a 2m LLAS

2.2.4 Low-frequency approximations

For low-frequencies (the flat region of the frequency response), the inductance of the 2 m LLAS is L_{LLA} = 7,92 µH (equation (3)).

Equation (11) becomes:

$$I_p = 0{,}0793 \cdot f_c(\omega) \cdot g_c(\omega) \cdot p_{EUT} \approx 0{,}066 \cdot p_{EUT} \tag{14}$$

or in dBs:

$$I_{LLA}\ (\text{dBµA}) = -23{,}3\ \text{dB} + p_{EUT}\ (\text{dBµAm}^2) \tag{15}$$

2.3 Sensitivity of an LLAS for different diameters

Equation (11) has been calculated for the different diameters of the LLAS given in Figure C.11 of CISPR 16-1-4. If the 2 m LLAS is taken as reference, the relative sensitivity can be calculated which replicates the results of Figure C.11. The result of this replication is given in Figure 5.

131 Tabular values of this Figure 5 are given in Table 1.

132

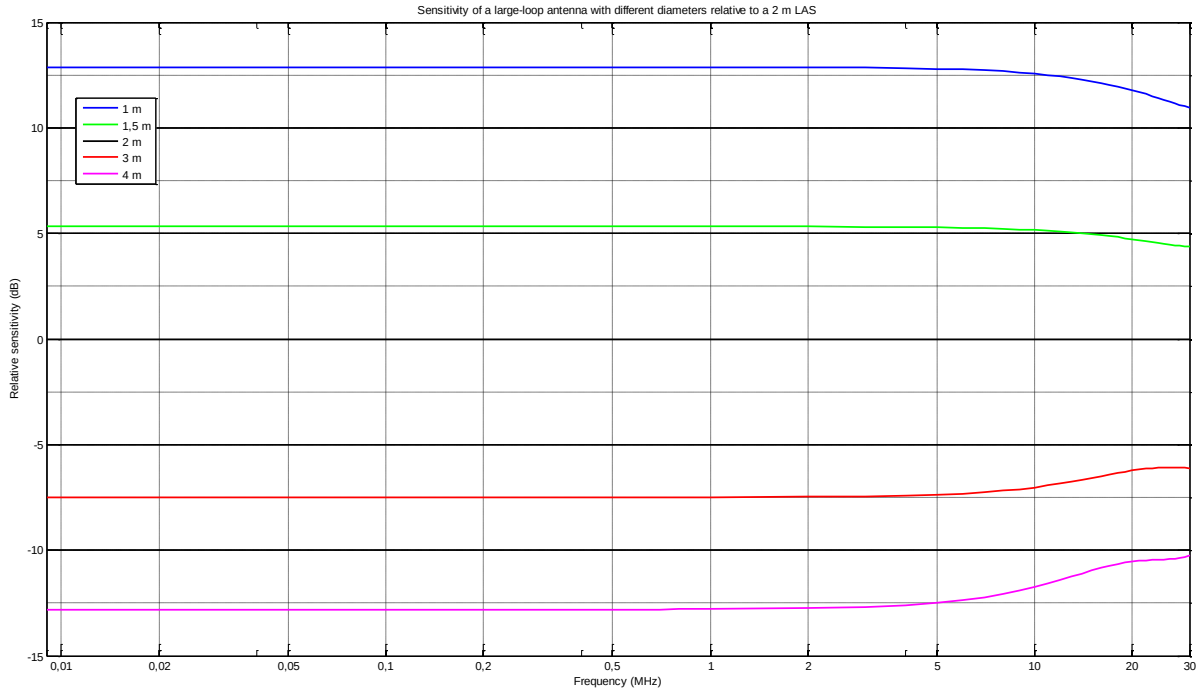

133

134 **Figure 5 – Replicated Figure C.11: Sensitivity of a large-loop antenna with diameter D**
135 **relative to a large-loop antenna having a diameter of 2 m**

136
137

Table 1 – Tabular values of the replicated Figure C.11 (Figure 5): sensitivity of a large-loop antenna with diameter *D* relative to a large-loop antenna having a diameter of 2 m

	LLAS diameter *D*					LLAS diameter *D*			
Frequency	1 m	1,5 m	3 m	4 m	Frequency	1 m	1,5 m	3 m	4 m
(MHz)	(dB)	(dB)	(dB)	(dB)	(MHz)	(dB)	(dB)	(dB)	(dB)
0,009	12,88	5,34	-7,5	-12,8	6	12,76	5,27	-7,31	-12,38
0,01	12,88	5,34	-7,5	-12,8	7	12,72	5,24	-7,25	-12,24
0,02	12,88	5,34	-7,5	-12,8	8	12,67	5,22	-7,18	-12,08
0,03	12,88	5,34	-7,5	-12,8	9	12,62	5,19	-7,11	-11,92
0,04	12,88	5,34	-7,5	-12,8	10	12,56	5,16	-7,02	-11,75
0,05	12,88	5,34	-7,5	-12,8	11	12,5	5,12	-6,94	-11,58
0,06	12,88	5,34	-7,5	-12,8	12	12,43	5,08	-6,85	-11,41
0,07	12,88	5,34	-7,5	-12,8	13	12,36	5,04	-6,76	-11,25
0,08	12,88	5,34	-7,5	-12,8	14	12,29	5	-6,67	-11,09
0,09	12,88	5,34	-7,5	-12,8	15	12,21	4,96	-6,58	-10,96
0,1	12,88	5,34	-7,5	-12,8	16	12,12	4,91	-6,5	-10,84
0,2	12,88	5,33	-7,5	-12,8	17	12,04	4,87	-6,42	-10,73
0,3	12,88	5,33	-7,5	-12,8	18	11,95	4,82	-6,35	-10,65
0,4	12,88	5,33	-7,5	-12,8	19	11,86	4,77	-6,28	-10,58
0,5	12,88	5,33	-7,5	-12,8	20	11,77	4,73	-6,23	-10,53
0,6	12,88	5,33	-7,5	-12,8	21	11,68	4,68	-6,18	-10,5
0,7	12,88	5,33	-7,5	-12,8	22	11,6	4,64	-6,14	-10,48
0,8	12,88	5,33	-7,49	-12,8	23	11,51	4,6	-6,11	-10,46
0,9	12,88	5,33	-7,49	-12,79	24	11,42	4,55	-6,09	-10,45
1	12,87	5,33	-7,49	-12,79	25	11,33	4,52	-6,08	-10,44
2	12,86	5,33	-7,48	-12,75	26	11,25	4,48	-6,08	-10,43
3	12,85	5,32	-7,45	-12,69	27	11,17	4,45	-6,08	-10,4
4	12,83	5,3	-7,41	-12,61	28	11,09	4,41	-6,09	-10,37
5	12,8	5,29	-7,37	-12,5	29	11,02	4,39	-6,1	-10,32
-	-	-	-	-	30	10,95	4,36	-6,12	-10,25

3 Response of LAS to the verification dipole

3.1 Relation LLAS-current and voltage applied to the balun dipole

The validation of the LLAS is carried out by measuring the current induced in the LLAS by the balun dipole specified in Clause C.5 of CISPR 16-1-4. See Figure 6. The balun dipole of width W and height H is fed with an RF generator with an open circuit voltage U_{go}. The measured current I_{ver} shall not deviate more than ±2 dB from the validation factor given in Figure C.8 of CISPR 16-1-4. The validation factor is:

$$\text{Validation factor} = 20\log\frac{U_{go}}{I_{ver}} \tag{16}$$

In this section the equation for validation factor given in Figure C.8 will be derived.

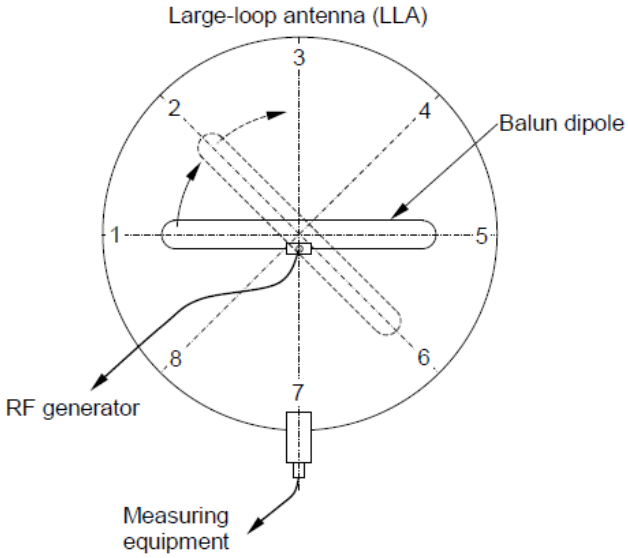

149

150 **Figure 6 – Setup of the balun dipole for verification of the LLAS**

151 **3.2 Calculation of mutual inductance: the simplified method**

152 The balun dipole is a folded dipole with semicircular ends. The mutual inductance M_{bd} of the
153 balun dipole with the LLAS can be calculated using equation (6) :

$$M_{bd} = \frac{\mu_0 S_{bd}}{D_{LLA}}, \tag{17}$$

154 where the surface S_{bd} of the balun dipole is:

$$S_{bd} = 1{,}4 \text{ m} \times 0{,}1 \text{ m} + (\pi \times 0{,}05^2) = 0{,}1479 \text{ m}^2. \tag{18}$$

155 The details of the construction of the balun dipole are given in Figure C.9 of CISPR 16-1-4.

156 For a 2m LLAS, the mutual inductance M_{bd} of the balun dipole is:

$$M_{bd}\,(\text{2m LLAS}) = 92{,}9 \text{ nH}. \tag{19}$$

157 This value of M_{bd} has been used originally [3] to calculate the present curve of the validation
158 factor given in CISPR 16-1-4 [2].

159 **3.3 Calculation of mutual inductance: the improved method**

160 The mutual inductance between the balun dipole and the large loop can be computed more
161 rigorously using the Neumann integral [5]:

$$M_{bd} = \frac{\mu_0}{4\pi} \oint_{C1} \oint_{C2} \frac{\vec{dl_1} \cdot \vec{dl_2}}{R_{12}}, \tag{20}$$

162 where R_{12} is the distance between the source point on the balun dipole and the observation point on
163 the large loop, and $\vec{dl_1}$ and $\vec{dl_2}$ are the differential path vectors as shown in Figure 7.

For a 2m LLA, the mutual inductance M_{bd} between the balun dipole and the LLAS computed is:

$$M_{bd}\,(2\text{m LLAS}) = 112{,}2\ \text{nH}. \tag{21}$$

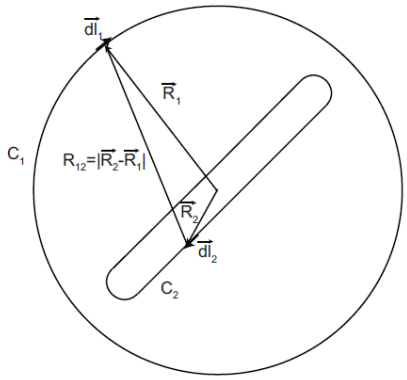

Figure 7 – Geometry model of LLA for numerical computation of Neumann integral [5]

3.4 Derivation of the equation for the validation factor

In this section, the analytical equation for the validation factor is replicated using the method given in [3][4][5]. In this method, the system comprising the LLAS and the balun dipole source is considered as a loosely coupled transformer.

The two halves of the folded dipoles may be represented by two pieces of short-circuited transmission line of length $W/2$ in series (Figure 8). The transmission line is comprised of two conductors at a distance of H = 0,1 m. The total impedance of the two transmission lines can be approximated by [7]:

$$Z_{bd} \approx 2Z_0 \tan(kW/2), \tag{22}$$

where Z_0 is the characteristic impedance of the two-wire transmission line given by:

$$Z_0 \approx 120\cosh^{-1}(H/d_{bd}), \tag{23}$$

Where d_{bd} is the outer diameter of the coaxial cable of the balun dipole. $Z_0 \approx 470\Omega$ for a two-wire transmission line with the centre of the wires at distance H = 0,1 m and for a diameter of each wire d_{bd} = 3,96 mm for RG-223/U.

As mentioned before, also these two coupled loops can be represented by a loosely coupled loop transformer. The total network representation of the generator, the balun dipole and the LLAS then can be represented as in Figure 9. From this figure it can be seen that the validation factor can be calculated as follows:

$$\text{Validation factor} = 20\log\left\{\frac{U_{go}}{I_{bd}} \cdot \frac{I_{bd}}{I_{ver}}\right\} \tag{24}$$

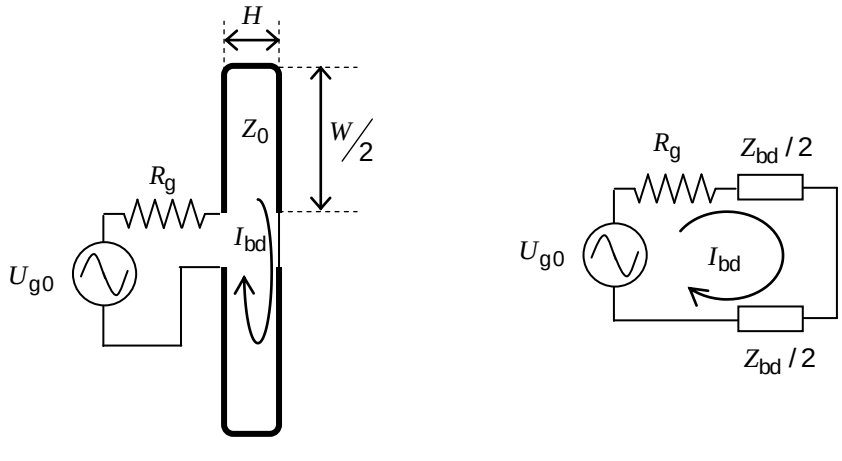

Figure 8 – Circuit representation of the balun dipole excluding the coupling effect from the LLAS

The ratio of the generator open voltage U_{go} and the current in the balun dipole I_{bd} follows from:

$$\frac{U_{go}}{I_{bd}} = R_g + Z_{bd} - \frac{j\omega M_{bd}^2}{L_{LLA}} \tag{25}$$

The ratio of the balun dipole current I_{bd} and the measured LLAS-current can be derived from equation:

$$\frac{I_{bd}}{I_{ver}} = \frac{L_{LLA}}{M_{bd} \cdot f_c(\omega) \cdot g_c(\omega)} \tag{26}$$

The validation factor defined in equation (24) then becomes:

$$\text{Validation factor} = 20\log\left\{\frac{L_{LLA}\left\{R_g + Z_{bd} - \dfrac{j\omega M_{bd}^2}{L_{LLA}}\right\}}{M_{bd} \cdot f_c(\omega) \cdot g_c(\omega)}\right\} \tag{27}$$

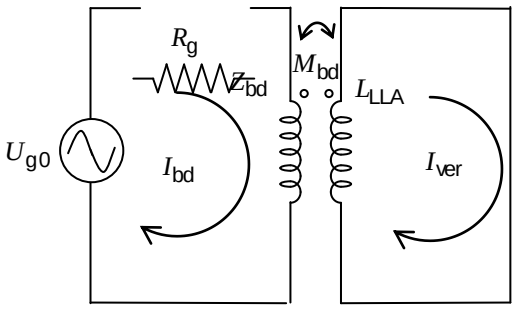

Figure 9 – Network model representation of the balun dipole fed by a generator source and the LLAS antenna

3.5 Replication of the current Figure C.8

The validation factor has been calculated for the LLAS of 2 m diameter using equation (27) and using the value of M_{bd} given in equation (19). The result is shown in Figure 10. This figure gives the same result as Figure C.8 of CISPR 16-1-4. The vertical axis of Figure 10 has been flipped.

Tabular values of this Figure 10 are given in Table 2.

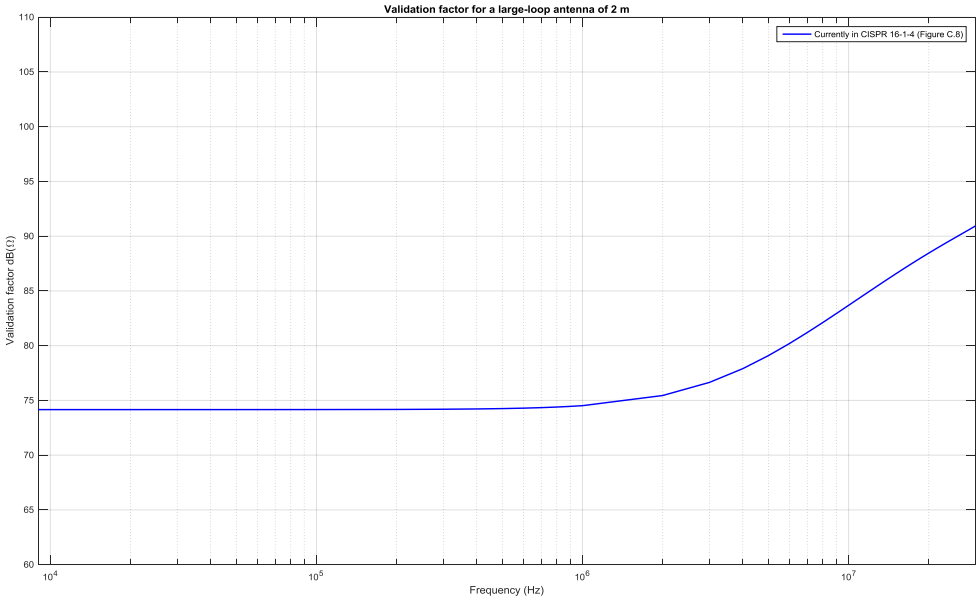

Figure 10 – Replicated Figure C.8: Validation factor for a large loop-antenna of 2 m diameter

229 **Table 2 – Tabular values of the replicated Figure C.8 (Figure 10)**

Frequency	Validation factor	Frequency	Validation factor
(MHz)	(dB)	(MHz)	(dB)
0,009	74,16	7	81,21
0,01	74,16	8	82,12
0,02	74,16	9	82,94
0,03	74,16	10	83,68
0,04	74,16	11	84,36
0,05	74,16	12	84,98
0,06	74,16	13	85,55
0,07	74,16	14	86,06
0,08	74,16	15	86,54
0,09	74,16	16	86,98
0,1	74,16	17	87,39
0,2	74,18	18	87,77
0,3	74,19	19	88,12
0,4	74,22	20	88,45
0,5	74,25	21	88,76
0,6	74,29	22	89,05
0,7	74,34	23	89,32
0,8	74,39	24	89,59
0,9	74,45	25	89,83
1	74,52	26	90,07
2	75,45	27	90,3
3	76,65	28	90,52
4	77,9	29	90,73
5	79,1	30	90,94
6	80,2	-	-

230

231 **3.6 Calculation of the new Figure C.8**

232 The new improved validation factor has been calculated for the LLAS of 2 m diameter using
233 equation (27) and using the more precise value of M_{bd} derived from the Neumann integral
234 given in equation (21). The result is shown in Figure 11. This figure shows a shift-down of the
235 curve of 1,64 dB with respect to the curve in Figure 10.

236 Tabular values of the new proposed validation curve given in Figure 11 are given in Table 3.

237

238 **Table 3 – Tabular values of the new Figure C.8 (Figure 11)**

Frequency (MHz)	Validation factor (dB)	Frequency (MHz)	Validation factor (dB)
0,009	72,52	7	79,57
0,01	72,52	8	80,47
0,02	72,52	9	81,30
0,03	72,52	10	82,04
0,04	72,52	11	82,72
0,05	72,52	12	83,34
0,06	72,52	13	83,90
0,07	72,52	14	84,42
0,08	72,52	15	84,90
0,09	72,52	16	85,34
0,1	72,52	17	85,75
0,2	72,54	18	86,13
0,3	72,55	19	86,48
0,4	72,58	20	86,81
0,5	72,61	21	87,12
0,6	72,65	22	87,41
0,7	72,70	23	87,68
0,8	72,75	24	87,94
0,9	72,81	25	88,19
1	72,88	26	88,43
2	73,81	27	88,66
3	75,01	28	88,88
4	76,26	29	89,09
5	77,46	30	89,30
6	78,56	-	-

239

240 The low-frequency asymptotic value of the new validation factor is:

$$\lim_{\omega \to 0} \text{Validation factor} = 20\log\left\{ \frac{L_{\text{LLA}} R_{\text{g}}}{M_{\text{bd}} \cdot \left(\frac{R_{\text{A}}}{R_{\text{A}} + R_{\text{C}} / v_{\text{c}}} \right)} \right\} = 72{,}52 \text{ dB} \tag{28}$$

241

242

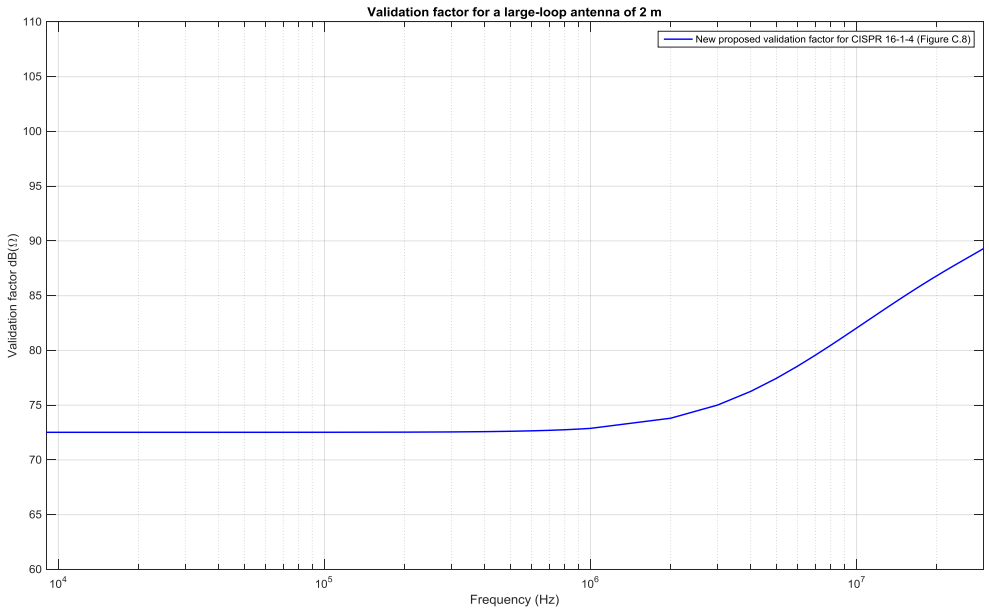

Figure 11 – New proposed Figure C.8: Validation factor for a large loop-antenna of 2 m diameter

3.7 NEC2 method

In [9] also a numerical method using NEC2 modelling has been applied, which gives slightly different results above 0,5 MHz because of the fact that at upper frequencies, the current distribution is not uniform anymore. It is acknowledged that the results between 0,5 MHz and 30 MHz are more accurate using the NEC2 method. However, the differences appear to be less than 0,13 dB (see Figure 12). For the purpose of standardization it is preferred to apply the analytical equation available that can readily be applied without the need for NEC2.

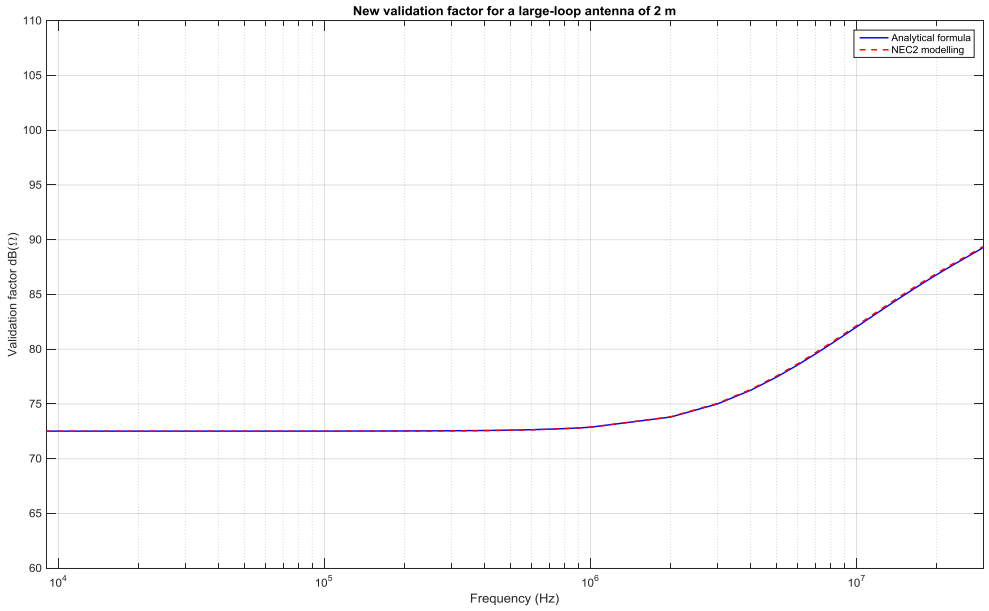

Figure 12 – Comparison analytical and numercal (NEC2) calculation

4 Magnetic field of a magnetic dipole above a ground plane

4.1 Model

Figure C.10 of CISPR 16-1-4 gives conversion factors for calculating the magnetic field from the current measured by a LLAS for a certain EUT at specified distances. The conversion factors given in Figure C.10 are taken over from the paper of Bergervoet [3]. In this chapter the equations for these conversion factors are given.

For the calculations the analytical equation for the magnetic field resulting from a magnetic dipole is used. Generally, the magnetic field vector $\boldsymbol{H}$ consists of three components H_x, H_y and H_z. It is assumed that the disturbance source in the EUT is represented by a magnetic dipole vector $\boldsymbol{p}$, whose magnitude is given by equation (1). See Figure 13.

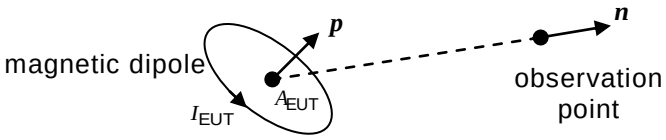

Figure 13 – Dipole moment of a small loop radiator in free space

The direction of this vector $\boldsymbol{p}$ is normal to the plane of the loop of the source current. In free space, the magnetic field vector $\boldsymbol{H}$ would be [6]:

$$\boldsymbol{H} = \frac{1}{4\pi}\left[k^2(\boldsymbol{n}\times\boldsymbol{p})\times\boldsymbol{n}\frac{e^{-jkr}}{r} + [3\boldsymbol{n}(\boldsymbol{n}\cdot\boldsymbol{p}) - \boldsymbol{p}]\cdot\left(\frac{1}{r^3} + \frac{jk}{r^2}\right)e^{-jkr}\right] \tag{29}$$

where

– $\boldsymbol{n}$ is the unit vector from the source to the observation point,

– r is the absolute value of the distance between the EUT and the observation point.

Equation (29) is the exact analytical description in free-space and contains the far-field part ($1/r$ - term) and the near-field and intermediate-field terms.

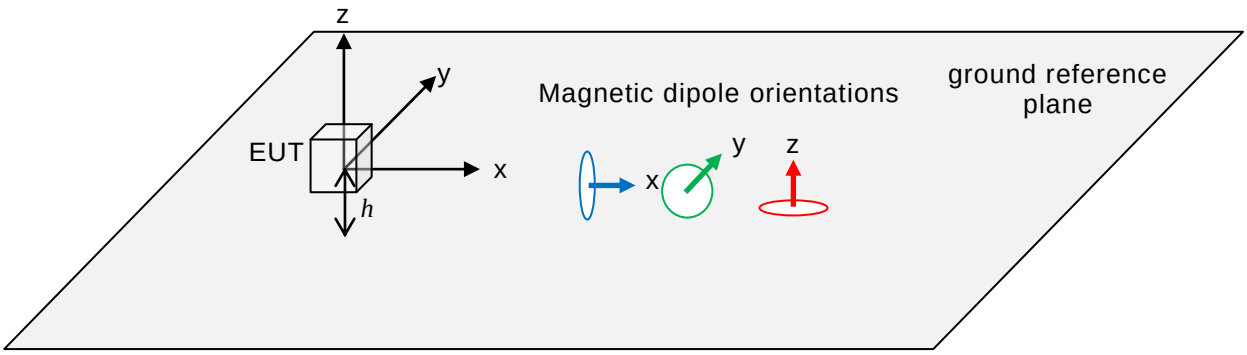

Figure 14 – EUT above a ground plane and the coordinate system and possible magnetic dipole orientations

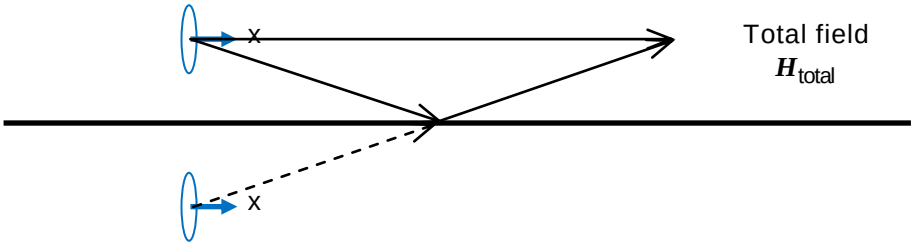

a. x-directed magnetic dipole

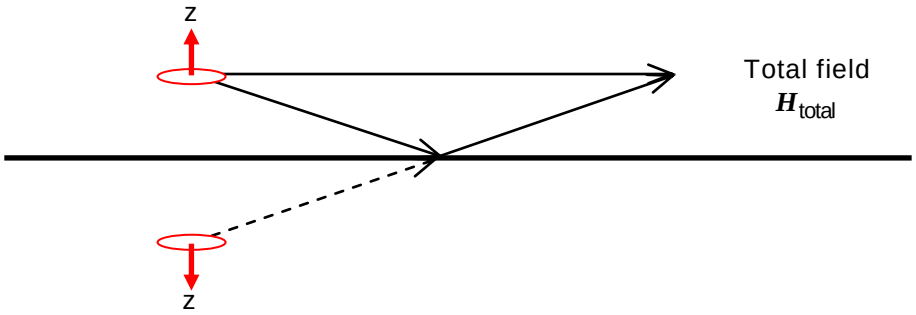

b. z-directed magnetic dipole

Figure 15 – Magnetic-field resulting from a source and its image below the ground plane (side view)

The position of the EUT at a height h above the ground reference plane and the associated x-y-z-coordinate system is depicted in Figure 14. The three possible orientations of the magnetic dipole inside the EUT are also given in Figure 14. It is assumed that the magnetic dipole is located above an ideally conductive ground plane (SAC or OATS). For calculating the total magnetic field, an additional mirror source has to be taken into account. Two examples of the way the direct source adds to the image source are given in Figure 15. In case of a horizontal x- or y-directed H-dipole, the dipole moment of the image has the same direction, which means that the image field adds to the direct field. The total field can be calculated by applying equation (29) twice:

$$\boldsymbol{H}_{\text{total}} = \boldsymbol{H}_{\text{direct}} + \boldsymbol{H}_{\text{image}} \tag{30}$$

For a vertical z-directed dipole (caused by a horizontal current loop) the image source has an opposite direction, which means that the direct field is weakened by its image field.

In this way the total magnetic field at a certain horizontal measurement distance r_{m} of a magnetic dipole above a ground reference planes has been calculated using Matlab.

4.2 Replication of Figure C.10

The three components H_x, H_y and H_z of the magnetic field of respectively three orthogonally oriented magnetic dipoles have been calculated for three horizontal distances. In order to replicate Figure C.10 of CISPR 16-1-4, the parameters of the configuration that has been published in [3] have been gathered from a Philips internal Technical Note [8]. These parameters are as follows:

– horizontal measurement distance r_{m} = 3, 10 and 30 m,

– height of the centre of the magnetic dipoles above the ground reference plane h = 1,3 m,

297 – height at which the magnetic field is calculated = 1,3 m,

298 – diameter magnetic dipole D = 0,4 m,

299 – current in the magnetic dipole loop I = 100 dBµA.

300 The results are shown in Figure 16 and Figure 17. Figure 16 gives the magnetic field
301 expressed in terms of dBµA/m. Figure C.10 of CISPR 16-1-4 also expresses the magnetic
302 field in terms of dBµV/m, simply by assuming that the free space impedance relation applies
303 (which is not the case). The magnetic field expressed in dBµV/m can be obtained by adding
304 the free-space impedance value:

$$Z_{\text{fs}} = 20\log(120\pi) = 51{,}5 \text{ dB}\Omega. \tag{31}$$

305 From these results we see that either the H_x or H_y component of respectively the x- and y-
306 directed dipole will lead to a high value. Therefore, the maximum value of the H_x or H_y
307 components are only of interest and have been determined [3]. These maximum values are
308 related to the current that would be measured by a 2 m LLAS for the same magnetic dipole.
309 This current is calculated using equation (13). The results are shown in Figure 18. This Figure
310 18 is the same as Figure C.10 of CISPR 16-1-4 with the exception that also the conversion
311 factor for 30 m distance is given. Note that the colours of the curves given in Figure 16,
312 Figure 17 and Figure 18 correspond with the colours of the magnetic dipoles shown in Figure
313 14.

314 Tabular values of the curves presented in Figure 18 are given in Table 4.

315 **4.3 Conversion factors for calculating magnetic field at other distances**

316 The result shown in Figure 18 can be used also to calculate conversion factors for calculating
317 the magnetic field at different distances. For instance if the magnetic field value is available at
318 3 m distance, the field at 10 m or 30 m can be obtained using the curves given in Figure 19.

319

320

321

322

323

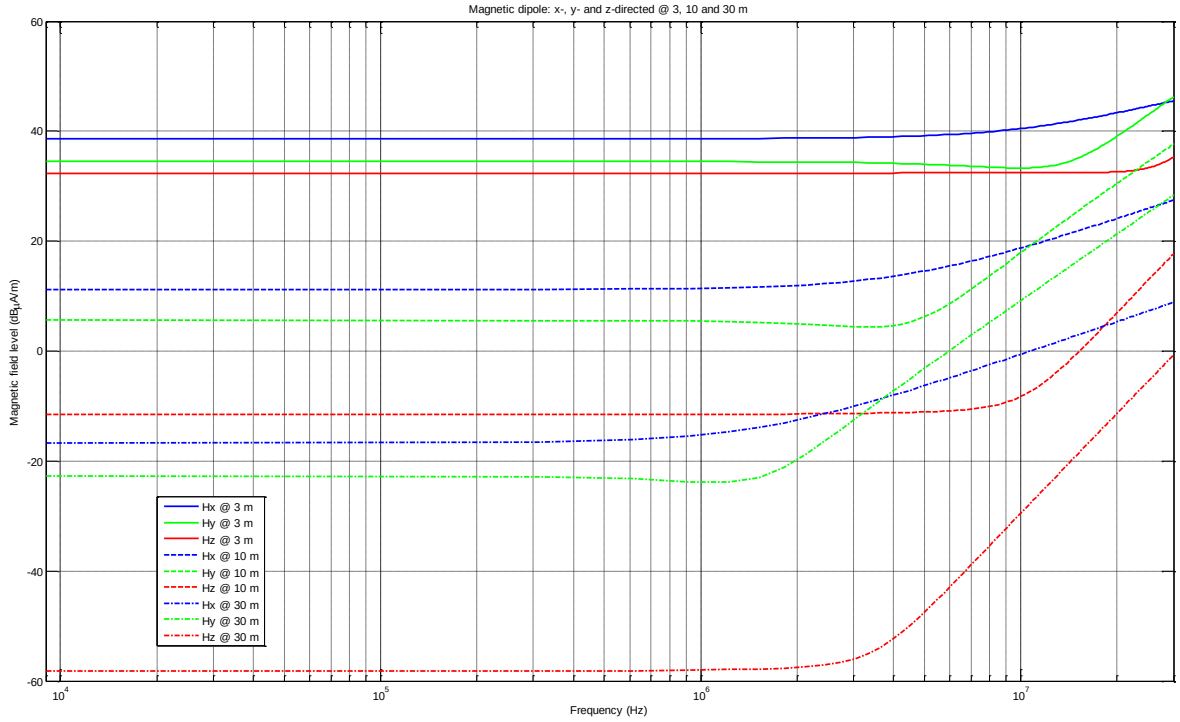

Figure 16 – Magnetic field (expressed in dBµA/m) of three dipole orientations at three distances

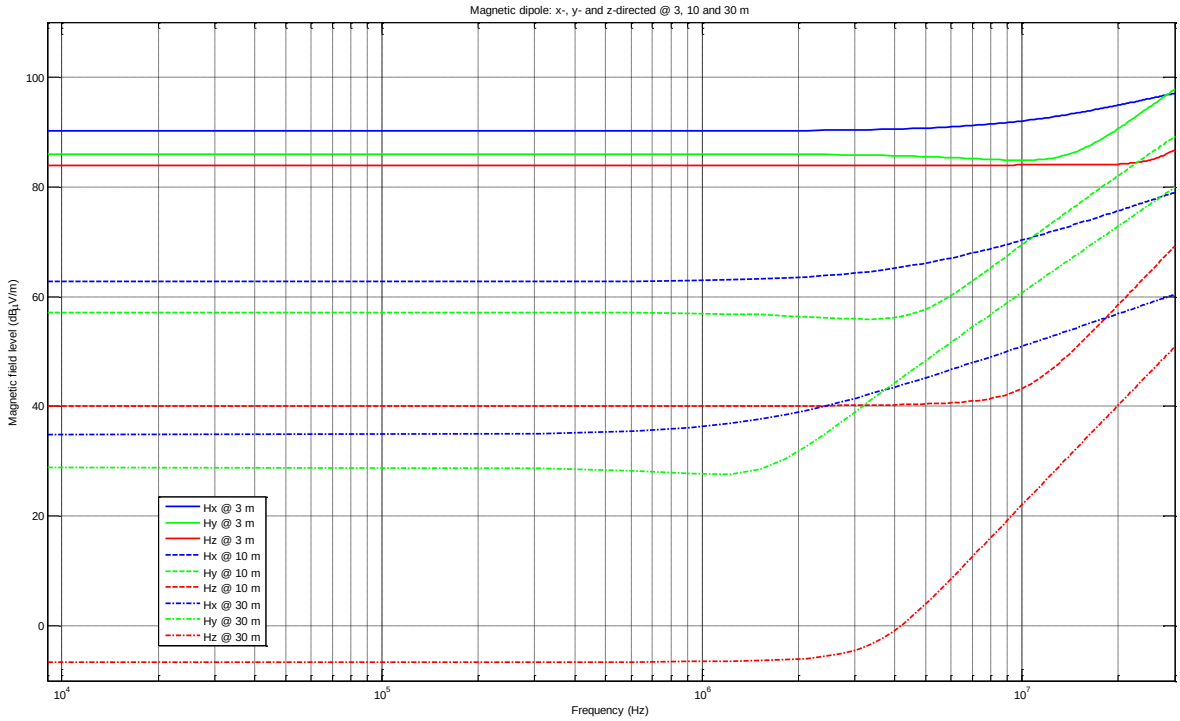

Figure 17 – Magnetic field (expressed in dBµV/m) of three dipole orientations at three distances

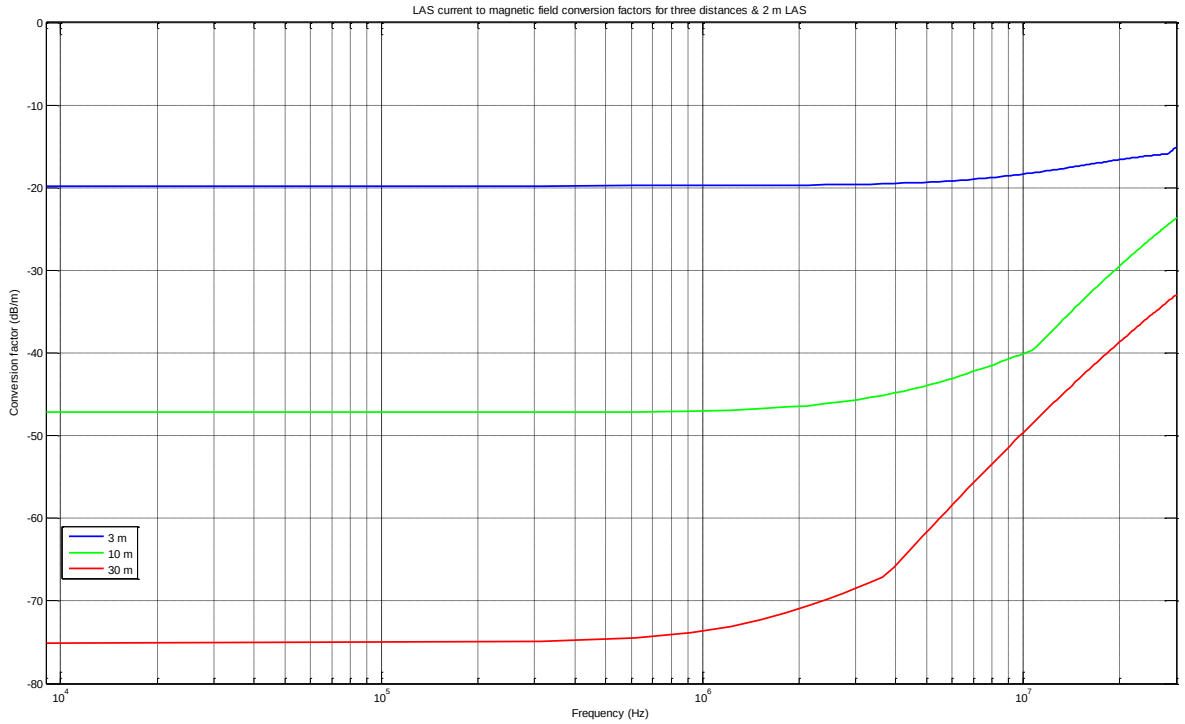

Figure 18 – Replicated Figure C.10: magnetic field conversion factors for three distances

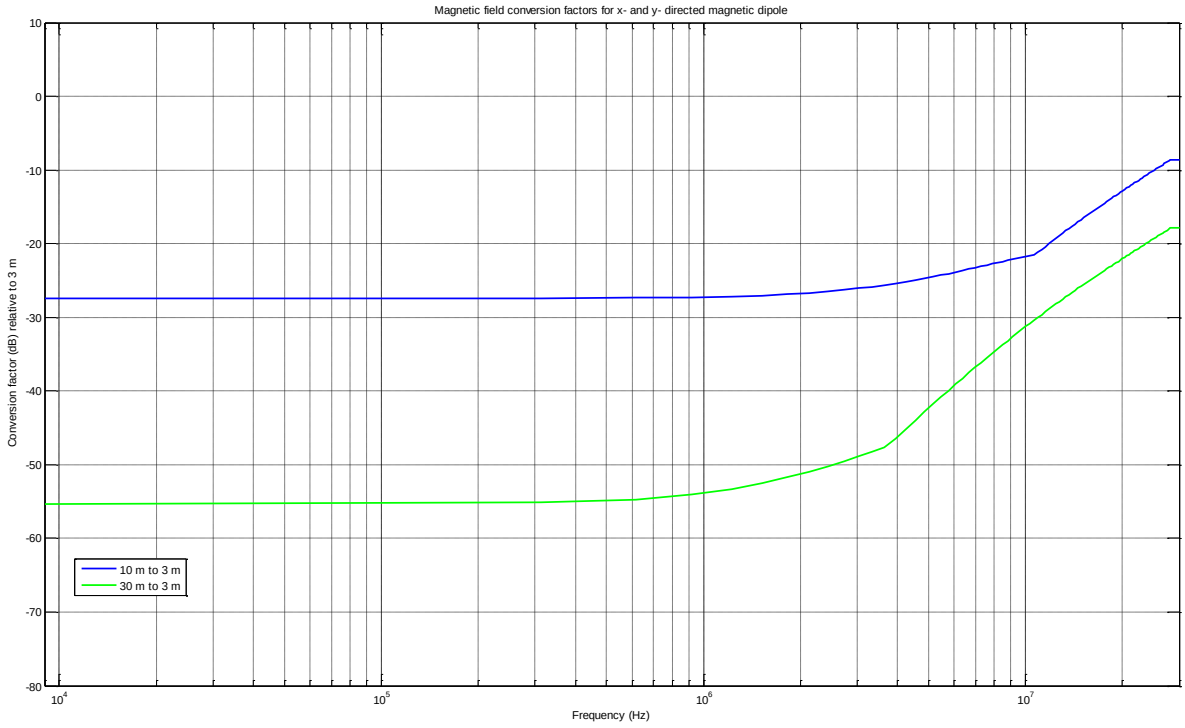

Figure 19 – Conversion factors for calculating magnetic field at 10 m or 30 m

338 **Table 4 – Tabular values of the replicated Figure C.10 (Figure 18)**

Frequency	2m LLAS to 3 m field	2m LLAS to 10 m field	2m LAS to 30 m field	Frequency	2m LLAS to 3 m field	2m LLAS to 10 m field	2m LAS to 30 m field
(MHz)	(dB/m)	(dB/m)	(dB/m)	(MHz)	(dB/m)	(dB/m)	(dB/m)
0,009	-19,77	-47,18	-75,09	7	-18,97	-42,23	-55,72
0,01	-19,77	-47,18	-75,09	8	-18,76	-41,45	-53,41
0,02	-19,77	-47,18	-75,09	9	-18,56	-40,74	-51,4
0,03	-19,77	-47,18	-75,09	10	-18,35	-40,08	-49,63
0,04	-19,77	-47,18	-75,09	11	-18,14	-39,24	-48,04
0,05	-19,77	-47,18	-75,08	12	-17,93	-37,72	-46,61
0,06	-19,77	-47,18	-75,08	13	-17,73	-36,36	-45,31
0,07	-19,77	-47,18	-75,08	14	-17,54	-35,11	-44,12
0,08	-19,77	-47,18	-75,08	15	-17,35	-33,97	-43,03
0,09	-19,77	-47,18	-75,08	16	-17,18	-32,92	-42,02
0,1	-19,77	-47,18	-75,07	17	-17,02	-31,95	-41,08
0,2	-19,77	-47,17	-75,02	18	-16,87	-31,05	-40,21
0,3	-19,77	-47,16	-74,94	19	-16,73	-30,22	-39,4
0,4	-19,77	-47,15	-74,82	20	-16,6	-29,44	-38,63
0,5	-19,76	-47,13	-74,68	21	-16,48	-28,71	-37,92
0,6	-19,76	-47,11	-74,51	22	-16,37	-28,02	-37,25
0,7	-19,76	-47,09	-74,32	23	-16,27	-27,37	-36,61
0,8	-19,76	-47,06	-74,11	24	-16,18	-26,76	-36,01
0,9	-19,75	-47,02	-73,88	25	-16,1	-26,18	-35,43
1	-19,75	-46,99	-73,64	26	-16,03	-25,62	-34,89
2	-19,69	-46,46	-70,97	27	-15,96	-25,1	-34,37
3	-19,6	-45,7	-68,52	28	-15,9	-24,59	-33,87
4	-19,48	-44,83	-65,7	29	-15,52	-24,11	-33,39
5	-19,33	-43,93	-61,65	30	-15,04	-23,64	-32,93
6	-19,15	-43,06	-58,41	-	-	-	-

339 ## 5 Change of LLAS validation criterion

340 Verification measurement results have been reported at the CISPR A WG1 meeting in Stresa
341 by Midori et al [9] and by Schwarzbeck [10].

342 Midori et al [9] reported verification test results using five existing LLAS systems in the
343 market. It was shown that the validation criterion of ±2 dB in the current CISPR 16-1-4
344 standard is very small due to design and manufacturing tolerances by of the LLAS and due to
345 the influence of the surrounding (floor) during the test.

346 In Mr. Schwarzbeck's paper [10], the average validation factor of 24 LLAS units is shown. The
347 24 LLAS unit have been exactly constructed according to the CISPR 16-1-4 specification. The
348 resulting average value is between the existing and new proposed validation factor curve.

349 Verification results reported by Mr. Midori et al in a later paper [11] shows that new proposed
350 validation curve with the 1,6 dB shift provides a better match with verification measurements
351 of actual LLAS units in the field (in the Japanese market). From these verification tests it was
352 also concluded that the current LLAS validation acceptance criterion of ±2 dB is hardly to
353 meet now in practice. Midori et al showed in [11] that the measurement uncertainty of the

LLAS validation test is 1,9 dB (expanded uncertainty). The variability due to construction tolerances and probe sensitivity uncertainty is 0,8 dB. Hence, the current LLAS acceptance criterion of ±2 dB is extremely tight.

As concluded already at the CISPR A WG1 meeting in Stresa, the reported LLAS verification test results justify the change of the acceptance criterion for the LLAS validation test from ±2 dB to ±3 dB.

6 Summary

This paper describes the models and equations of the Large Loop Antenna System that are needed to determine the curves given in Figure C.8, Figure C.10 and Figure C.11 of CISPR 16-1-4 [2] . Also the tabular values of the curves are given. The curve for the validation factor (Figure C.8) has been improved. Also the justification for changing the LLAS validation criterion from ±2 dB to ±3 dB is given.

Annex A gives the proposed changes in Annex C of CISPR 16-1-4 that are needed to incorporate the tabular values of the curves in question.

In replicating the curves, an in view of the increased relevance of magnetic field measurement methods below 30 MHz, it is proposed to add parts of this paper also as background material in CISPR TR 16-3.

7 References

[1] CISPR/A/WG1 LAS tables (Beeckman)15-01, *LAS model and tabular values of LLA figures in Annex C of CISPR 16-1-4*, 2015-01-21.

[2] CISPR 16-1-4: 2012-07 (ed. 3.1), *Specification for radio disturbance and immunity measuring apparatus and methods – Part 1-4: Radio disturbance and immunity measuring apparatus – Antennas and test sites for radiated disturbance measurements*.

[3] J.R. Bergervoet, H. van Veen, *A Large-Loop Antenna for Magnetic Field Measurements*, Proceedings of the 8th International Zürich Symposium on Electromagnetic Compatibility, March 1989, ETH Zentrum - IKT, 8092 Zürich, Switzerland, p. 29-34.

[4] J. McLean, H. Sako, A. Medina, R. Sutton, *Operation of the Van Veen Loop in a shielded chamber*, Instrumentation and Measurement Technology Conference (I2MTC), May 2013.

[5] J. McLean, K. Takizawa, M. Midori, H. Kurihara, R. Sutton, *The Effects of Asymmetry on the operation of the Van Veen Loop*, Proc. of the 2014 International Symposium on Electromagnetic Compatibility (EMC Europe 2014), Gothenburg, Sweden, September 1-4, 2014.

[6] J.P. Jackson, *Classical electrodynamics*, John Wiley & Sons, 3rd edition.

[7] S. Ramo, J.R. Whinnery, T. Van Duzer, *Fields and Waves in Communication Electronics*, Wiley.

[8] H. van Veen, *Correlation between maximum magnetic field strengths and transmitter distances*, Philips Lighting Central Development Laboratories Technical Note VLc TM 2037/87, 1987-08-21.

[9] CISPR/A/WG1 LAS Tables (Midori-McLean-Kurihara-Fujii-Shinozuka)15-02, *Proposal of tabular values of validation factor and conversion factor for LAS*, August 2015.

[10] CISPR A WG1 paper Schwarzbeck (Stresa meeting 2015), Loop Antenna System CISPR 16-1-4 Ed. 3.

[11] CISPR/A/WG1 LAS Tables (Midori-Kurihara-Fujii-Shinozuka)15-04, *Verification of the calculation model of validation factor and the tolerance of validation factor for LAS*, January 2016.

Annex A

Changes required in CISPR 16-1-4 ed. 3.1

3.2 Abbreviations

Replace

LAS loop antenna system

by

LLAS large loop antenna system

4.7 Special antenna arrangements – Loop antenna system

Replace in the title and text of subclause 4.7

Loop antenna system *or* LAS

by

large loop antenna system *or* LLAS

Annex C

Replace throughout Annex C

loop antenna system *or* LAS

by

large loop antenna system *or* LLAS

C.4 Validation of a large-loop antenna (LLAS)

3rd paragraph, change the tolerance of validation factor; replace:

±2 dB

by

±3 dB

Add the following paragraph at the end of subclause C.4

Tabular values of the curves presented in Figure C.8 and Figure C.11 are given in respectively Table C.1 and Table C.2. Background material and the equations for calculating the validation factor are given in CISPR 16-3 [xx].

Add Table 3 of this paper as a new Table C.1.

Replace Figure C.8 by Figure 11 of this paper.

Figure C.9 needs to be modified in the following way.

In Figure C.9 a note shall be added that the indicated distances are cable centre to cable centre distances:

NOTE Distances indicated are cable centre to cable centre distances

In Figure C.9 the dimension of the bending radius 5 cm is to be added.

C.6 Conversion factors

In the first paragraph, replace

(see Figure C.10) *by* (see Figure C.10 and Table C.2)

Add the following sentence at the end of the first paragraph:

Background material and the equations for calculating these conversions are given in CISPR 16-3 [xx].

Add after the first paragraph the following statement

The validation of the LLAS shall be performed at the location where the LLAS measurements normally take place. This is to account for the effect of the floor, walls and similar objects or surfaces in the environment of the LLAS.

In the first paragraph, replace

(see Figure C.11)

by

(see Figure C.11 and Table C.3)

Replace Figure C.10 by Figure 18 of this paper.

Replace Figure C.11 by Figure 5 *of this paper.*

Replace the 5th paragraph

In general, the conversion factor is frequency-dependent; Figure C.10 presents C_{dA} for standardized distances of 3 m and 10 m. For the standardized distance d = 30 m, the conversion factor is under consideration.

by

In general, the conversion factor is frequency-dependent; Figure C.10 (and Table C.2) presents C_{dA} for standardized distances of 3 m, 10 m and 30 m.

Add Table 4 of this paper as a new Table C.2.

Add Table 1 of this paper as a new Table C.3.

Bibliography

Add CISPR 16-3 as reference (provided that the background material and equations as presented in this paper are included).

[xx] CISPR TR 16-3: 20xx, *Specification for radio disturbance and immunity measuring apparatus and methods - Part 3: CISPR technical reports*